Stress-Induced Nanoparticle Crystallization

Huimeng Wu,[†,||] Zhongwu Wang,[‡] and Hongyou Fan*[,†,§]

[†]Advanced Materials Laboratory, Sandia National Laboratory, Albuquerque, New Mexico 87106, United States
[‡]Cornell High Energy Synchrotron Source, Wilson Laboratory, Cornell University, Ithaca, New York 14853, United States
[§]NSF Center for Micro-Engineered Materials, Department of Chemical and Nuclear Engineering, The University of New Mexico, Albuquerque, New Mexico 87131, United States

S *Supporting Information*

ABSTRACT: We demonstrate for the first time a new mechanical annealing method that can significantly improve the structural quality of self-assembled nanoparticle arrays by eliminating defects at room temperature. Using *in situ* high-pressure small-angle X-ray scattering, we show that deformation of nanoparticle assembly in the presence of gigapascal level stress rebalances interparticle forces within nanoparticle arrays and transforms the nanoparticle film from an amorphous assembly with defects into a quasi-single crystalline superstructure. Our results show that the existence of the hydrostatic pressure field makes the transformation both thermodynamically and kinetically possible/favorable, thus providing new insight for nanoparticle self-assembly and integration with enhanced mechanical performance.

Precise engineering of periodic nanoparticle superstructures (so-called artificial solids or materials) attracts a lot of attention because of their promise for optical, electronic, and magnetic devices.[1−5] The integration of engineered nanoparticle materials is expected to be highly sensitive to structural factors, such as interparticle spacing and degree of long-range order, requiring the development of robust self-assembly with controlled nanoparticle aggregations over macroscopic length scales. To date, engineering of nanoparticle assemblies has relied mainly on specific interparticle chemical or physical interactions, such as van der Waals forces, electrostatics, dipole−dipole interactions, DNA-hybridization, etc.[6]

Previous work by us, as well as others, has shown nanoparticle self-assembly to result generally in polycrystalline 2- or 3D close-packed arrangements through balancing interparticle forces at ambient conditions.[4,7−11] These nanoparticle assemblies often exhibit defects such as random packed domains, grain boundary, and vacancy that are lack of continuous pathway for electron or energy transfer. Efforts have been made to achieve "single crystal-like" domain structures with precise long-range order for their definite advantages for electron or energy transfer. For example, solvent and thermal annealing methods were developed to form long-range ordered nanoparticle superlattices.[12,13] Thermal annealing and solvent vapor annealing, although accelerate structural relaxation and induce grain growth, do not significantly improve the crystal quality of nanoparticle films due to either sintering of nanoparticles or remaining of film cracking.

Heterogeneous precipitation method was also reported,[14] enabling fabrication of well-shaped supercrystal solids. These works were all conducted under ambient pressure. Things change much and differently under high external pressure.[5,15−18] Under high-pressure conditions, the free-energy change of the materials system (due to the PV term in the Gibbs free energy $G = E + PV − TS$) may allow a new opportunity to tune phase or configuration of the materials, which inspires us to study how external pressure (or stress) makes influence of nanoparticle self-assembly.

In this work, we present experimental studies to demonstrate a new mechanical annealing method that can significantly improve the structural quality of self-assembled nanoparticle arrays by eliminating the defects and inducing orientated crystallization at room temperature. Using *in situ* high-pressure small-angle X-ray scattering (HP-SAXS), we show that pressure-induced annealing of nanoparticle assembly in the presence of ~6 GPa hydrostatic pressure rebalances interparticle forces within nanoparticle arrays and transforms the nanoparticle film from an amorphous assembly with defects into a quasi-single crystalline superstructure. Our results demonstrate that the existence of a hydrostatic high-pressure field makes the transformation both thermodynamically and kinetically possible/favorable.

The platform for the mechanical annealing studies is a diamond anvil cell (DAC).[19] The materials system for our studies comprises gold nanoparticles capped with an organic monolayer of alkane chains and their ordered films that were formed through rapid evaporation of gold nanoparticle solutions. Samples of gold nanoparticle thin films were loaded into a DAC. Silicone oil was used as a pressure transmitting medium to produce hydrostatic pressure field within the DAC. Pieces of ruby crystal were added together with the gold nanoparticle sample so that the pressure inside the DAC chamber can be ascertained by probing the shifts of the pressure-dependent ruby fluorescence peaks (see details in Supporting Information).

During experiments, we raised the pressure gradually to start the compression process followed by releasing back to ambient pressure. Each pressure data point was collected between 5 and 10 min. Synchrotron-based HP-SAXS measurements were performed to monitor directly the *in situ* structural evolution. Representative HP-SAXS images and integrated SAXS

spectrum of the gold nanoparticle film collected during compression and release course are shown in Figures 1 and
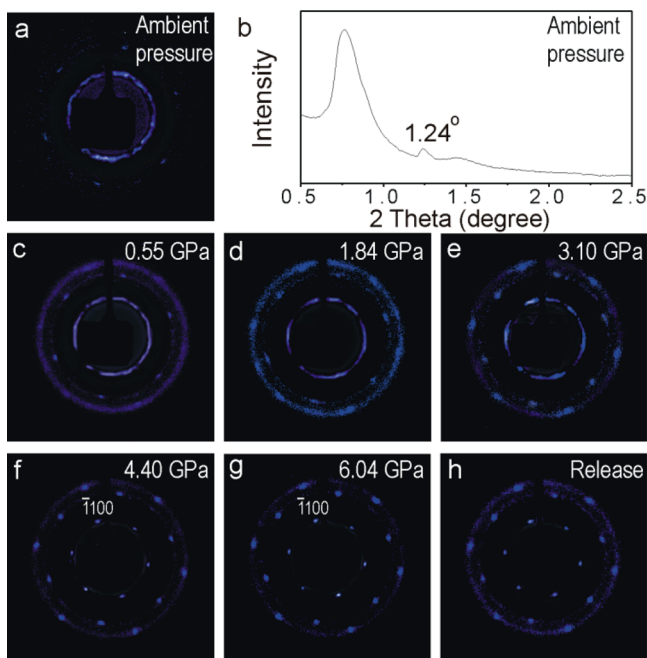

Figure 1. Structural evolution of gold nanoparticle arrays upon pressurization. (a) A representative HP-SAXS image of gold nanoparticle arrays at ambient pressure. (b) SAXS pattern integrated from image in (a). SAXS patterns of the gold nanoparticle arrays during compression (c–g) and release (h).

2. The SAXS images and integrated patterns demonstrate that the nanoparticle assemblies gradually evolve from a mixture of small clusters with fcc, hcp, and amorphous phases into a quasi-single crystalline hcp structure. At ambient pressure, the SAXS image shows that the sample has a polycrystalline phase and consists of intermixing of small size of domains (or clusters) of fcc, hcp, and disordered phases. As the pressure in the DAC increases, the sample simultaneously experiences the deformation due to the compression. At ambient pressure, the SAXS diffraction intensity is weak. No obvious diffraction is visible outside the six symmetrical diffraction spots at $2\theta = 1.24°$, which indicates the small size of the crystalline domains or clusters. At 0.55 GPa, a new Debye–Scherrer diffraction ring appears at $2\theta = 1.46°$, accompanied by significant increase in diffraction intensity of all peaks (Figure 2a,b). The appearance of this diffraction signalizes the increase of domain size in the film. When the pressure is increased to 1.84 GPa, a set of six spots starts to arise on this third Debye–Scherrer ring. With continuous increase of pressure, the first diffraction ring gradually fuses into the six-spotty texture, suggesting a large hcp crystalline domain is growing at expense of others. This is also reflected on the integrated SAXS pattern, where the shoulder peak 2 due to fcc {002} shrinks continuously (Figure 2). For pressure higher than 4.4 GPa, the SAXS pattern becomes all single-crystal diffraction spots, which strongly suggests that the sample has entirely transformed into a large single hcp domain with [0001] orientation. The fact that the orientation of the diffraction pattern matches perfectly with the diffraction spots observed at ambient pressure (Figure 1a) is a strong evidence that the final hcp single crystal structure grows from the initial hcp domains (Figure S1). Figure 2b shows the
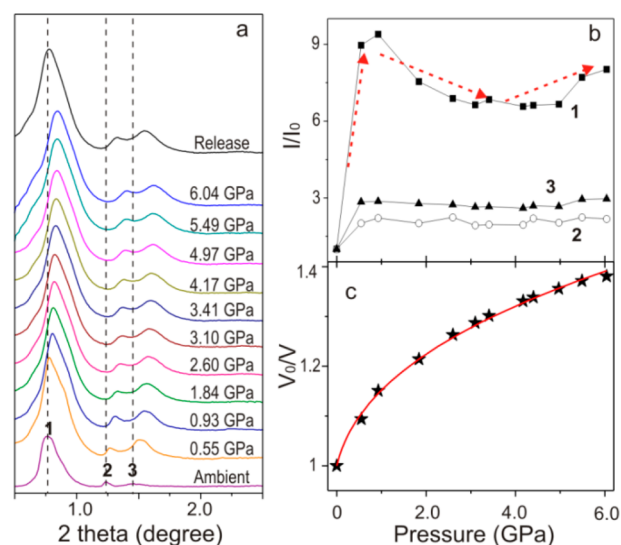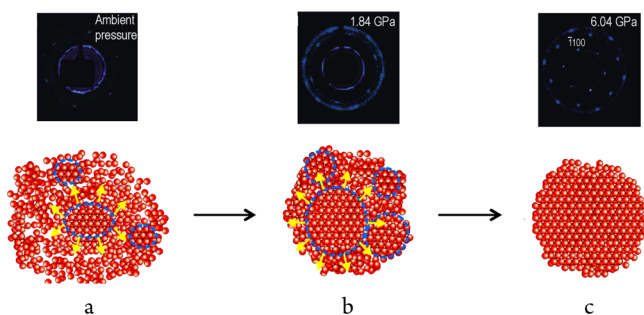

Figure 2. Structural development of gold nanoparticle arrays and formation of a quasi-single crystalline gold nanoparticle assembly under high-pressure annealing. (a) HP-SAXS spectra integrated from SAXS patterns of nanoparticle arrays collected during compression and release. (b) Ratio of intensities of the Bragg peaks to that at ambient pressure (I/I_0) upon increasing pressure. (c) Volume ratio (V_0/V) upon increasing pressure. Black stars represent experimental data; red dashed line represents a fit of Birch–Murnaghan EOS.[20] K_0 is the bulk modulus, K' is its pressure derivative $(K' = dK_0/dP)$, and V and V_0 are the unit cell volumes at pressure and initial volume before compression. Fitting the compression data gave $K_0 = 2.5$ GPa and $K' = 17.6$.

relative intensity change of the first Bragg peak as a function of pressure to that at ambient pressure. The significant increase (>9 fold) of peak intensities (from ambient pressure to 0.93 GPa) indicates that application of pressure facilitates the growth of the small domains of crystalline clusters and simultaneous reduction of random nanoparticles in the gold film. Following that, the intensity starts to decrease slightly with the further increase of pressure. This may be affected by the reduced thickness of the sample under compression. When the pressure was increased to around 4 GPa, the intensity begins to increase again with the increase of pressure. This increase of intensity comes from the highly ordered gold assemblies. These experimental results clearly demonstrate that the high-pressure field leads to significant improvement in structural quality of the nanoparticle assembly. Fitting the compression data (Figure 2c) shows a bulk modulus close to those of organic ligand matrix and polymer.[21]

The observed mechanical annealing phenomena can be explained by a pressure-driven close packing process of nanoparticles (Scheme 1). The starting self-assembled nanoparticle film consists of structural defects including vacancy, random packed domains, and grain boundaries and is thus not at a minimum energy state. The external compression first eliminates the vacancy by structural shrinkage that is evidenced by the significant volume shrinkage during compression course (Figure 2c). The van der Waals interactions from the soft interdigitating alkane chains provide essential/certain mobility and allow local nanoparticles rearrangement under stress. The applied stress breaks the original force balance within the nanoparticle assembly and makes the nanoparticles prone to structural rearrangements. Meanwhile, the applied pressure compresses the nanoparticle assembly toward a new force-

Scheme 1. Schematic Illustration for the Formation of Pressure-Induced Annealing and Crystallization of Gold Nanoparticle Supercrystals[a]

[a](a) At ambient pressure, nanoparticle arrays with defects and randomly packed small clusters. (b) Upon increasing pressure, defects are gradually removed and nanoparticle assemblies start to re-arrange. Ordered crystal domains as a template lead to growth of larger nanoparticle crystals. (c) Formation of single-crystalline nanoparticle superlattices.

balanced, more close-packed configuration. During this process, the crystalline domains will consume the random packed smaller domains and grow larger, similar to the Ostward ripen mechanism. As there is a large pre-existed [0001] oriented hcp domain in the starting nanoparticle film, this domain serves as the initial structural template and grows into a sample-wide, quasi-single crystalline structure.

In summary, we observed the pressure-induced super-crystallization of nanoparticle arrays. Under a continuous hydrostatic pressure up to ~6 GPa, randomly packed gold nanoparticle arrays gradually transit to quasi-single crystalline hcp structure. HP-SAXS results show that the deformation of nanoparticle assemblies under stress rebalances interparticle forces within nanoparticle arrays and transforms the nanoparticle film from an amorphous assembly with defects into a quasi-single crystalline superstructure. Our mechanical annealing study constitutes the first observation of room temperature, pressure-induced grain growth in nanoparticle system, and provides a simple and efficient way to improve the structural quality of nanoparticle assembly with enhanced mechanical strength.

■ ASSOCIATED CONTENT

Ⓢ Supporting Information

Experimental methods of nanoparticle synthesis and self-assembly at ambient pressure and high-pressure crystallization and characterization and electron diffraction patterns of ordered gold nanoparticle arrays. This material is available free of charge via the Internet at http://pubs.acs.org.

■ AUTHOR INFORMATION

Corresponding Author

hfan@sandia.gov

Present Address

∥Carl Zeiss Microscopy, LLC, 1 corporation way, Peabody, MA 01960.

Notes

The authors declare no competing financial interest.

■ REFERENCES

(1) Alivisatos, A. P. *Science* **1996**, *271*, 933.
(2) Andres, R. P. *Science* **1996**, *273*, 1690.
(3) Collier, C. P.; Saykally, R. J.; Shiang, J. J.; Henrichs, S. E.; Heath, J. R. *Science* **1997**, *277*, 1978.
(4) Fan, H. Y.; Yang, K.; Boye, D. M.; Sigmon, T.; Malloy, K. J.; Xu, H. F.; Lopez, G. P.; Brinker, C. J. *Science* **2004**, *304*, 567.
(5) Quan, Z.; Wang, Y.; Bae, I.-T.; Loc, W. S.; Wang, C.; Wang, Z.; Fang, J. *Nano Lett.* **2011**, *11*, 5531.
(6) Min, Y.; Akbulut, M.; Kristiansen, K.; Golan, Y.; Israelachvili, J. *Nat. Mater.* **2008**, *7*, 527.
(7) Dunphy, D.; Fan, H.; Li, X.; Wang, J.; Brinker, C. J. *Langmuir* **2008**, *24*, 10575.
(8) Wright, A.; Gabaldon, J.; Burckel, D. B.; Jiang, Y.-B.; Tian, Z. R.; Liu, J.; Brinker, C. J.; Fan, H. *Chem. Mater.* **2006**, *18*, 3034.
(9) Murray, C. B.; Kagan, C. R.; Bawendi, M. G. *Science* **1995**, *270*, 1335.
(10) Sun, Y. G.; Xia, Y. N. *Science* **2002**, *298*, 2176.
(11) Wang, Z.; Schliehe, C.; Bian, K.; Dale, D.; Bassett, W. A.; Hanrath, T.; Klinke, C.; Weller, H. *Nano Lett.* **2013**, *13*, 1303.
(12) Hanrath, T.; Choi, J. J.; Smilgies, D.-M. *ACS Nano* **2009**, *3*, 2975.
(13) Korgel, B.; Zaccheroni, N.; Fitzmaurice, D. *J. Am. Chem. Soc.* **1999**, *121*, 3533.
(14) Talapin, D. V.; Shevchenko, E. V.; Kornowski, A.; Gaponik, N.; Haase, M.; Rogach, A. L.; Weller, H. *Adv. Mater.* **2001**, *13*, 1868.
(15) Grochala, W.; Hoffmann, R.; Feng, J.; Ashcroft, N. W. *Angew. Chem., Int. Ed.* **2007**, *46*, 3620.
(16) Wang, Z.; Schliehe, C.; Wang, T.; Nagaoka, Y.; Cao, Y. C.; Bassett, W. A.; Wu, H.; Fan, H.; Weller, H. *J. Am. Chem. Soc.* **2011**, *133*, 14484.
(17) Wu, H.; Bai, F.; Sun, Z.; Haddad, R. E.; Boye, D. M.; Wang, Z.; Huang, J. Y.; Fan, H. *J. Am. Chem. Soc.* **2010**, *132*, 12826.
(18) Guo, Q.; Zhao, Y.; Mao, W. L.; Wang, Z.; Xiong, Y.; Xia, Y. *Nano Lett.* **2008**, *8*, 972.
(19) Mao, H. K. *Science* **1978**, *200*, 1145.
(20) Fei, Y.; Ricolleau, A.; Frank, M.; Mibe, K.; Shen, G.; Prakapenka, V. *Proc. Natl. Acad. Sci. U. S. A.* **2007**, *104*, 9182.
(21) Podsiadlo, P.; Lee, B.; Prakapenka, V. B.; Krylova, G. V.; Schaller, R. D.; Demortiere, A.; Shevchenko, E. V. *Nano Lett.* **2011**, *11*, 579.